



<http://www.diva-portal.org>

## Postprint

This is the accepted version of a paper presented at *2017 IEEE MTT-S International Microwave Symposium*.

Citation for the original published paper:

Glubokov, O., Xinghai, Z., Beuerle, B., Champion, J., Shah, U. et al. (2017)  
Micromachined Multilayer Bandpass Filter at 270 GHz Using Dual-Mode Circular Cavities.  
In:  
<https://doi.org/10.1109/MWSYM.2017.8058894>

N.B. When citing this work, cite the original published paper.

Permanent link to this version:

<http://urn.kb.se/resolve?urn=urn:nbn:se:kth:diva-217394>

# Micromachined Multilayer Bandpass Filter at 270 GHz Using Dual-Mode Circular Cavities

Oleksandr Glubokov, *Member*, Xinghai Zhao, *Student Member*, Bernhard Beuerle, *Student Member*, James  
Campion, *Student Member*, Umer Shah, *Member*, and Joachim Oberhammer, *Senior Member, IEEE*

Micro- and Nanosystems, School of Electrical Engineering, KTH Royal Institute of Technology, Stockholm  
SE-100 44, Sweden

**Abstract**— In this paper, we present a microfabricated fourth-order sub-THz WR-3.4 bandpass waveguide filter based on  $TM_{110}$  dual-mode circular-shaped cavity resonators. The filter operates at the center frequency of 270 GHz with fractional bandwidth of 1.85% and two transmission zeros are introduced in the upper and in the lower stopband using a virtual negative coupling. The microchip filter is significantly more compact than any previous dual-mode designs at comparable frequencies, occupying less than 1.5 mm<sup>2</sup>. Furthermore, in contrast to any previous micromachined filter work, due to its axially arranged interfaces it can be directly inserted between two standard WR-3.4 rectangular-waveguide flanges, which vastly improves system integration as compared to previous micromachined filters; in particular no custom-made split-block design is required. The cavities are etched in the handle layer of a silicon-on-insulator (SOI) wafer, and coupling is realized through rectangular slots fabricated in the SOI device layer. Couplings of the degenerate modes in one cavity are facilitated by means of small perturbations in the circular cavity shapes. The measured average return loss in the passband is  $-18$  dB and worst-case return loss is  $-15$  dB, and an insertion loss of only 1.5 dB was measured. The excellent agreement between measured and simulated data is facilitated by fabrication accuracy, design robustness and micromachined self-alignment geometries.

**Index Terms**— waveguide filters, dual-mode filters, microfabrication, micromachining technology.

## I. INTRODUCTION

In recent years, applications in sub-THz frequency bands have been attracting increasing attention. Frequency selective circuits, in particular bandpass filters, remain one of the most important components in wireless system architectures. Since fabrication of resonating devices at high frequencies requires high precision geometrical features for good performance and in particular for high product uniformity without post-fabrication tuning, photolithographic-based micromachining, even allowing for MEMS reconfigurability [1-2], is an excellent fabrication technology for higher-order complex filters at sub-THz frequencies. Several micromachined examples of direct-coupled and cross-coupled bandpass filters designed for sub-THz frequency range have been reported [3-7]; all of them require a custom-made split-block assembly to connect with standard waveguide flanges. Recently, in [8], a micromachined multilayer cross-coupled filter had been implemented for Ka-band; however even for this 10-times lower frequency than in the present paper, and despite using micromachining,

that design was not very robust resulting in detuning and shifting of the response with a relatively poor 8 dB return loss.

Dual-mode filters based on two degenerate  $TE_{111}$  modes in circular waveguide cavities have been known since the 1970s [9]. Evolution of the dual-mode filter design techniques eventually led to a series of works on filters exploiting square-shaped cavities with two TM degenerate modes:  $TM_{120}$  and  $TM_{210}$  [10-12]; in these papers, it has been shown that a large variety of pseudo-elliptic responses can be obtained by connecting dual-mode cavities in series and through non-resonating nodes. Moreover, the TM-cavities have an important advantage: they are very compact in the direction of propagation and their compactness is only limited by required Q-factors and power handling. Filters of these classes require accurate post-fabrication tuning usually performed by screws, which is very difficult to realize at sub-THz frequencies. In [4], a micromachined pseudo-elliptic filter has been designed using two cascaded elliptic-shaped cavities with quasi- $TM_{110}$  resonances at 400 GHz. It has been shown that at sub-THz frequencies  $TM_{110}$  circular and elliptic cavities exhibit higher unloaded Q-factors than square and rectangular single and dual-mode cavities, and thus are better suitable for filters. At the same time, the dual-mode cavities have larger dimensions and therefore are less sensitive to fabrication tolerances.

In this work, we present a narrowband fourth-order sub-THz filter with two transmission zeros in upper and lower stopbands. Our filter uses two dual-mode  $TM_{110}$  circular-shaped cavities arranged on three micromachined silicon chips with coupling apertures in-between the chips. This device class requires high-precision alignment of the adjacent layers, which is addressed by micromachined self-alignment structures on the chips. We also minimize sensitivity of the flange-to-filter coupling by connecting the flange directly to the input aperture. Thereby, we obtain a compact filter occupying minimum area on a chip without a need to include additional waveguide feedlines to its input/output ports, as well as sophisticated transitions or specially fabricated metal holders required for their characterization and operation. To our best knowledge, this is the first micromachined sub-THz filter which enables direct axial flange mounting. Experimental results are demonstrated to prove feasibility of the proposed design and the highly accurate fabrication.

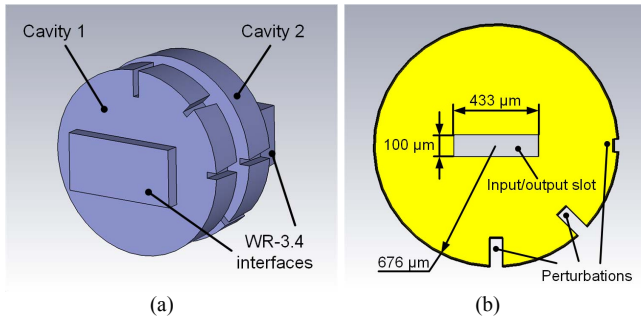


Fig. 1. Schematic view of the fourth-order dual-mode cavities filter: (a) perspective 3D-model view; (b) transversal cross-section view of a single cavity.

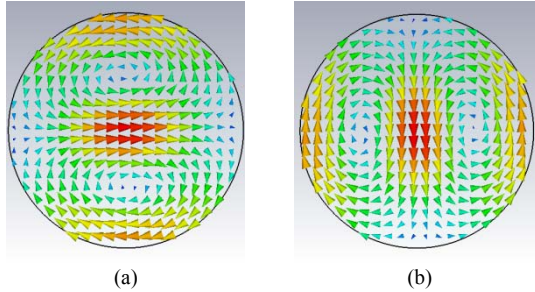


Fig. 2. Magnetic field distribution in dual-mode  $TM_{110}$  circular cavities at resonances: (a) horizontally polarized mode; (b) vertically polarized mode.

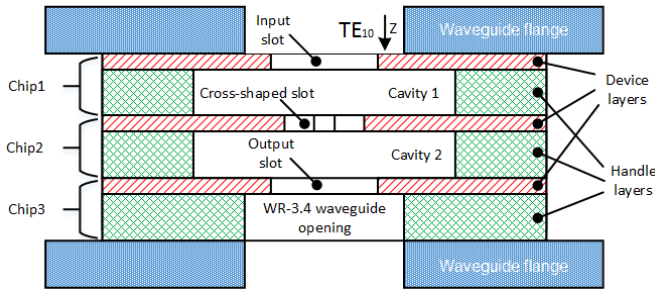


Fig. 3. Longitudinal cross-section view of the proposed 3-layer micromachined filter axially inserted between two waveguide flanges.

## II. DUAL-MODE FILTER DESIGN

In Fig. 1, a perspective view (Fig. 1a) and a single cavity transversal cross-section view (Fig. 1b) of the designed band-pass filter are presented. The filter contains two circular cavities, each accommodating a pair of degenerate  $TM_{110}$  modes (see Fig. 2) with vertically and horizontally polarized magnetic fields, internal perturbations in the cavities, several slots to realize internal and external couplings, as well as a waveguide opening. The longitudinal structure of the filter is shown in Fig. 3. External coupling is created through horizontal slots between the feeding waveguides and resonators. Interaction between the cavities is facilitated by orthogonally arranged coupling slots forming a cross-shaped aperture. The perturbations made inside the dual-mode resonators generate asymmetry in the cavities, thus tuning resonance frequencies of the degenerate modes: the vertical perturbation tunes the horizon-

tally polarized mode, while the horizontal perturbation adjusts the vertically polarized mode. The perturbations arranged at  $45^\circ$  angle create a coupling between the two orthogonal modes in the cavity.

Consequently, the principle of the filter's operation can be summarized as follows: initially, a  $TE_{10}$  mode propagating in the feeding rectangular waveguide excites a horizontally polarized  $TM_{110}$  mode in the Cavity 1; then, a vertically polarized  $TM_{110}$  mode is excited in Cavity 1 through the  $45^\circ$ -perturbation; next, the resonating fields in Cavity 1 launch both degenerate modes in Cavity 2 by the magnetic field interaction through the cross-shaped slot; after that, the two modes in Cavity 2 interact via the  $45^\circ$ -perturbation which is rotated clockwise by  $90^\circ$  with respect to the center of the cavity in order to create a virtual negative coupling between the vertically polarized modes in both resonators through the cross-shaped slot; and finally, the horizontally polarized mode in Cavity 2 excites a  $TE_{10}$  mode in the output rectangular waveguide.

The filter was designed and optimized in CST Microwave Studio with respect to the following specifications:

- (1) center frequency:  $f_0 = 270$  GHz;
- (2) ripple passband:  $f_{min} \dots f_{max} = 267.5 \dots 272.5$  GHz;
- (3) maximum return loss in passband:  $RL = -20$  dB;
- (4) minimum out-of-band rejection:  $A = 30$  dB below 264 GHz and above 276 GHz.

## III. FABRICATION

The complete filter assembly consists of three stacked chips: two with the waveguide cavities, input and coupling slots (top and middle chips) and a bottom chip with the output slot and the waveguide opening (see Fig. 3). A photograph of a single-layer chip and the final chip, containing multiple test filters is shown in Fig. 4.

Alignment of the chips to be stacked is extremely important for this type of filter. Therefore, several micromachined self-alignment features are implemented on the chips.

The size of the entire chip with 5 test filters, including waveguide-flange alignment holes is  $20 \times 8$  mm<sup>2</sup>. The area occupied on the chip by a single filter is determined by the cavity's radius and is approx. 1.5 mm<sup>2</sup>.

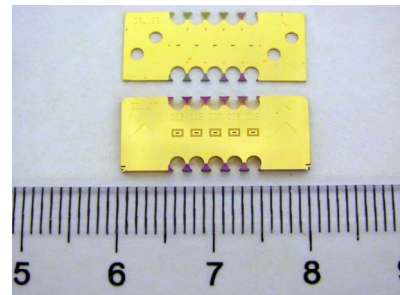


Fig. 4. Photograph of a single chip (top) and a completely assembled filter chip (bottom).

The chips are fabricated in a four-mask micromachining process using an SOI wafer covered with a silicon dioxide layer on the both sides acting as photolithography hard-masks. The resonating cavities are etched by deep-reactive ion etching (DRIE) of the handle layer (275- $\mu\text{m}$  thick) using a modified BOSCH-process; next, the coupling apertures are fabricated in the device layer (30- $\mu\text{m}$  thick) using the same process. The filter has been carefully designed in EM-simulator taking into account the expected side-wall profile of the etching process evaluated from test fabrication runs. Each chip is metallized by sputtering a 1- $\mu\text{m}$  thick layer of gold.

The assembly of the three layers happens on chip level. The average misalignment of the assembly has been calculated to be about 2  $\mu\text{m}$ . Finally, the three stacked chips are bonded together through thermo-compression bonding.

#### IV. MEASUREMENT AND RESULTS

For characterization, the filter chips were placed between standard WR-3.4 waveguide flanges and measured using a Rohde&Schwarz ZVA24 vector network analyzer with two ZC330 millimeter-wave converters for 220 to 330 GHz. Calibration is done at the waveguide flanges. A photograph of the measurement setup with a filter chip between two standard WR-3.4 waveguide pieces is shown in Fig. 5.

Fig. 6 shows simulated and measured results of the dual-mode circular cavity filter.

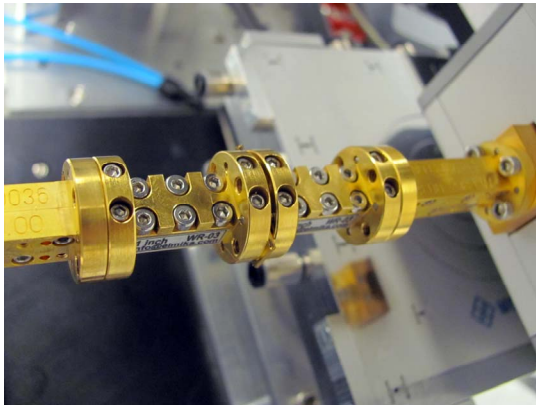


Fig. 5. Measurement setup showing a filter chip inserted between two standard WR-3.4 waveguide flanges.

It is visible from Figure 6 that the simulated and measured results are in excellent agreement. The best measured insertion loss in the passband is  $IL = 1.27$  dB, while the average value is  $IL_{ave} = 1.5$  dB. The measured worst-case return loss in the passband is  $RL = -15$  dB, and the average return loss in the passband is  $RL_{ave} = -18$  dB. This difference in return loss to the designed  $-20$  dB is assumed to be attributed to slight misalignment of the three layers of the chip.

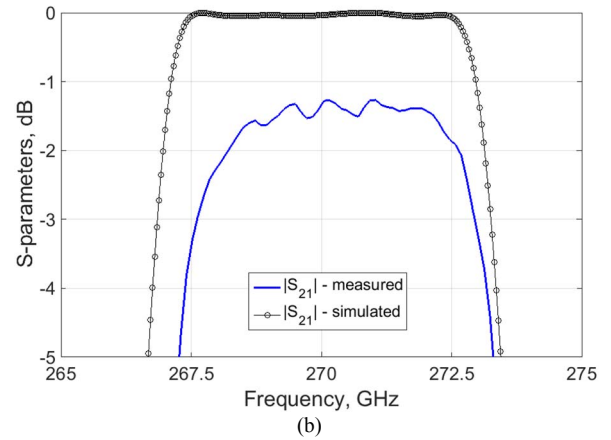
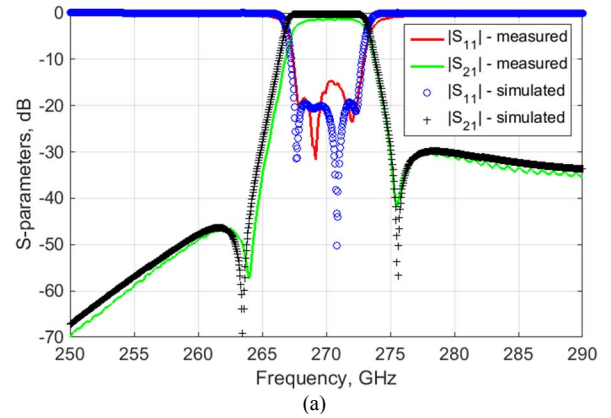


Fig. 6. Measured and simulated data showing excellent agreement: (a) S-parameters of the filter; (b) close-up view of insertion loss in the passband.

#### V. CONCLUSION

A micromachined multilayer bandpass filter based on two dual-mode circular cavities operating at the center frequency of 270 GHz has been presented. The filter has been designed taking into account the information regarding estimated deviation of the lateral walls from the vertical positions due to non-uniform etching. The presented experimental results show excellent agreement with the simulations, which confirms that micromachining is an excellent fabrication technology for high-performance, highly-accurate and compact filter implementations at sub-THz frequencies.

#### ACKNOWLEDGMENT

This work has been funded by The Swedish Foundation for Strategic Research through the Synergy Grant Electronics SE13-007, and by the European Research Council (ERC) through the Consolidator Grant No. 616846.

## REFERENCES

- [1] U. Shah *et al.*, "Submillimeter-Wave 3.3-bit RF MEMS Phase Shifter Integrated in Micromachined Waveguide," *IEEE Trans. THz Science and Tech.*, vol. 6, no. 5, pp. 706-715, Sept 2016.
- [2] U. Shah, T. Reck, H. Frid, C. Jung-Kubiak, G. Chattopadhyay, I. Mehdy, and J. Oberhammer, "A 500-750 GHz RF MEMS Waveguide Switch," *IEEE Trans. THz Science and Tech.*, vol. 7, no. 3, May 2017 (accepted, to be published).
- [3] X. Shang, M. Ke, Y. Wang and M. J. Lancaster, "WR-3 Band Waveguides and Filters Fabricated Using SU8 Photoresist Micromachining Technology," *IEEE Trans. Terahertz Science and Tech.*, vol. 2, no. 6, pp. 629-637, Nov. 2012.
- [4] J. x. Zhuang, Z. C. Hao and W. Hong, "Silicon Micromachined Terahertz Bandpass Filter With Elliptic Cavities," in *IEEE Trans. Terahertz Science and Tech.*, vol. 5, no. 6, pp. 1040-1047, Nov. 2015.
- [5] X. H. Zhao *et al.*, "D-Band Micromachined Silicon Rectangular Waveguide Filter," *IEEE Microwave and Wireless Comp. Letters*, vol. 22, no. 5, pp. 230-232, May 2012.
- [6] C. A. Leal-Sevillano *et al.*, "Silicon Micromachined Canonical E-Plane and H-Plane Bandpass Filters at the Terahertz Band," in *IEEE Microwave and Wireless Comp. Letters*, vol. 23, no. 6, pp. 288-290, June 2013.
- [7] J. Hu, S. Xie and Y. Zhang, "Micromachined Terahertz Rectangular Waveguide Bandpass Filter on Silicon-Substrate," in *IEEE Microwave and Wireless Components Letters*, vol. 22, no. 12, pp. 636-638, Dec. 2012.
- [8] P. Farinelli, L. Pelliccia, B. Margesin and R. Sorrentino, "Ka-band surface-mountable pseudo-elliptic filter in multilayer micromachined technology for on-board communication systems," in *2016 IEEE MTT-S Int. Microw. Symp. Dig.*, San Francisco, CA, 2016, pp. 1-4.
- [9] A. E. Williams, "A four-cavity elliptic waveguide filter," *IEEE Trans. Microw. Theory Tech.*, vol. 18, no. 12, pp. 1109-1114, Dec. 1970.
- [10] S. Bastioli, C. Tomassoni and R. Sorrentino, "TM dual-mode pseudoelliptic filters using nonresonating modes," *2010 IEEE MTT-S Inter. Microw. Symp.*, Anaheim, CA, 2010, pp. 880-883.
- [11] S. Bastioli, C. Tomassoni and R. Sorrentino, "A New Class of Waveguide Dual-Mode Filters Using TM and Nonresonating Modes," in *IEEE Trans. Microw. Theory Tech.*, vol. 58, no. 12, pp. 3909-3917, Dec. 2010.
- [12] C. Tomassoni, S. Bastioli and R. Sorrentino, "Generalized TM Dual-Mode Cavity Filters," in *IEEE Trans. Microw. Theory Tech.*, vol. 59, no. 12, pp. 3338-3346, Dec. 2011.